Progress In Electromagnetics Research M, Vol. 58, 147–157, 2017

Design and Measurement of a Novel Seamless Scanning Leaky Wave Antenna in Ridge Gap Waveguide Technology

Xingchao Dong[1, 2, *], Hongjian Wang[1, 2], Fei Xue[1, 2], and Yang Liu[1, 2]

Abstract—The design and measurement of a novel seamless scanning leaky wave antenna in ridge gap waveguide technology are presented. The impedance matching technique is employed to eliminate the open-stopband (OSB) effect which produces a discontinuity for a seamless scanning leaky wave antenna. Ridge gap waveguide proposed recently is used as the feed structure. The antenna radiates from longitudinal slots of which the leakage constant is designed small to ensure a high directivity. Subsequently, for simplicity, a transition from Ku-band standard waveguide port (WR62) to ridge gap waveguide is designed, which operates within Ku-band with S_{11} below -15 dB. A prototype has been fabricated, and measurements support the simulations obtained by full-wave analysis. The proposed antenna bandwidth is from 12.5 GHz to 17.4 GHz while seamless scanning is achieved from backward to forward, particularly including broadside radiation. The scanning range is from $-9°$ to $19°$ with an average gain of 18.3 dB.

1. INTRODUCTION

Leaky wave antenna (LWA) has exhibited attractive advantages in wide ranges such as broadband wireless communication, collision-avoidance radar, frequency modulated continuous wave radar, and pattern synthesis [1, 2]. Generally, the scanning range is considered specially since it is necessary for practical applications [3]. A high directivity of the LWA is also needed for positioning accurately. These can be realized by periodic loading of the same components on each unit cell of the LWA, and hence leads to a high directivity and a beam scanning ability. The open-stopband (OSB) may occur when the beam is scanned through broadside, which blocks the continuous scanning from backward to forward as the frequency increases [4]. This can be explained by that the reflected waves of each unit cell are in phase at the frequency of broadside radiation. Consequently, no electromagnetic wave is fed into the LWA for broadside radiation. To overcome this difficulty, reflection cancellation, impedance matching, implementing asymmetric unit cells and the balanced composite right/left-handed (CRLH) transmission line [5–8] have been adopted. Recently, a novel seamless scanning substrate integrated waveguide (SIW) LWA based on impedance matching technique is proposed. The periodic arrangement of the transverse and longitudinal elements can suppress the OSB completely [9].

Compared to SIW [10, 11], ridge gap waveguide (RGW) is a novel transmission line, which is first proposed in 2009 [12]. RGW resembles the parallel plate waveguide and the difference is that one of the plates is provided with a textured surface realized by bed of nails, which forms a high impedance boundary referred to as artificial magnetic conductor (AMC) [13, 14]. The AMC boundary prohibits fields from propagating in any directions in the gap except a confined gap wave propagating along a ridge. Theoretical principles and experimental verification are carefully performed in [15, 16]. RGW characterizes its simple mechanical assembly, low losses, wider bandwidth compared to rectangular

Received 18 May 2017, Accepted 5 July 2017, Scheduled 17 July 2017
* Corresponding author: Xingchao Dong (jtmsrcnn@163.com).
[1] Key Laboratory of Microwave Remote Sensing, National Space Science Center, China. [2] University of Chinese Academy of Sciences, Beijing, China.

waveguide. Many applications in gap waveguide technology such as power divider, filter, coupler, and slot antenna have been realized [17–22].

There are a few papers involving the combination between LWA and gap waveguide. A novel gap waveguide leaky wave antenna has been reported in [23]. The proposed leaky wave antenna structure is integrated into a groove gap waveguide transmission line. By designing different stopbands formed by both sides of the transmission line, fields can be radiated. A long slot array antenna in RGW technology is presented in [24]. Non-resonance radiating long slots are introduced in the designed array antenna. Two different techniques are adopted to mitigate the grating lobe and enhance the antenna gain. However, the combination between LWA based on impedance matching technique and RGW has not existed in the literature according to the authors' knowledge. Therefore, the paper aims at presenting a novel seamless scanning LWA based on impedance matching technique in RGW technology. Therein, a transition is designed so as to acquire better combination from standard rectangular waveguide (WR62) port to the RGW transmission line. Moreover, a prototype is fabricated to verify the initial thought.

2. IMPEDANCE MATCHING TECHNIQUE

As a rule, leaky wave antenna with a high directivity can be designed by periodic loading of the same components on each unit cell. The unit cell can be realized by a transverse slot or a longitudinal slot located on the broad wall of a rectangular waveguide. This arrangement also makes the antenna have a frequency-dependent scanning ability. As mentioned above, the OSB effect will be encountered inevitably which deteriorates antenna performances, so additional techniques should be adopted to suppress this effect for seamless scanning. Here, we introduce the impedance matching technique proposed in [9], first of all, a simple description is given below.

Figure 1(a) describes the LWA unit cell structure located on the broad wall of a rectangular waveguide. The unit cell consists of a transverse slot as a series inductance and a longitudinal slot as a shunt capacitance. Since the antenna is a kind of travelling-wave antennas, two ports are added at both ends, one is the power input port and the other is the matching port. According to the transmission line theory, its equivalent circuit is shown in Fig. 1(b). In Fig. 1(b), Z_0 is the characteristic impedance of the transmission line, the transverse slot is equivalent to the series impedance Z and the longitudinal slot is equivalent to the shunt admittance Y.

Based on microwave network theory, if the circuit is matching, Y can be derived as

$$Y = \frac{Z}{Z0(Z0 - Z)} \tag{1}$$

When the circuit is matching, the return loss is very small, which means that the power flowing the slots can be radiated. Therefore, the OSB effect can be avoided by using the impedance matching technique. The OSB effect suppression can be inferred if the broadside radiation is observed, and the return loss is small.

Figure 1. Periodic slots located on the broad wall of a rectangular waveguide, (a) periodic unit cell structure; (b) the equivalent circuit of the unit cell.

3. ANTENNA DESIGN

LWA is an important class of traveling-wave antennas, of which planar periodic slots located on a grounded substrate are utilized to radiate electromagnetic wave. It is very essential to know the complex propagation constant for governing the design.

The main lobe direction of leaky wave antenna is mainly determined by the phase constant, which is frequency-dependent. It describes the scanning capability of leaky wave antenna and can be predicted simply as

$$\theta_m = \sin^{-1}(\beta/k_0) \tag{2}$$

where k_0 is the free-space wavenumber. The phase constant β can be determined using classical formula for metallic rectangular waveguide as

$$\beta = \sqrt{\varepsilon_r k_0^2 - (\pi/w_{eff})^2} \tag{3}$$

where w_{eff} is the effective width of the RGW, which cannot be estimated by simple formula currently. It may be larger or smaller than the width of RGW.

The attenuation constant α can be determined as [25]

$$\alpha = -\frac{1}{2L} \ln\left(|S_{11}|^2 + |S_{21}|^2\right) \tag{4}$$

where L is the aperture length of the LWA.

3.1. Geometry of the Proposed Antenna

The structure of the proposed LWA is shown in Fig. 2. A dielectric substrate (Rogers 5880) is filled within the gap between the ridge line and the top metallic plate. A specific gap can be ensured and the relative permittivity of the substrate ($\varepsilon_r = 2.2$) is small for at least dielectric loss. The height of the substrate is set to 1 mm and the ridge width is set to 4 mm respectively. The period of the unit cell is 15.5 mm, about one waveguide wavelength at 14 GHz. Longitudinal slots are alternately arranged on both sides of the centerline to reduce the cross-polarization level, and transverse slots are also employed as explained in Section 2. Metal pins are located between the substrate and the bottom plate, and there are three row metal pins on both sides respectively, which can be used as shielded walls to avoid the lateral field leakage. Two waveguide ports are utilized, one is the feed and the other is the matching port to absorb residual power. The fabricated antenna prototype is presented in Fig. 3.

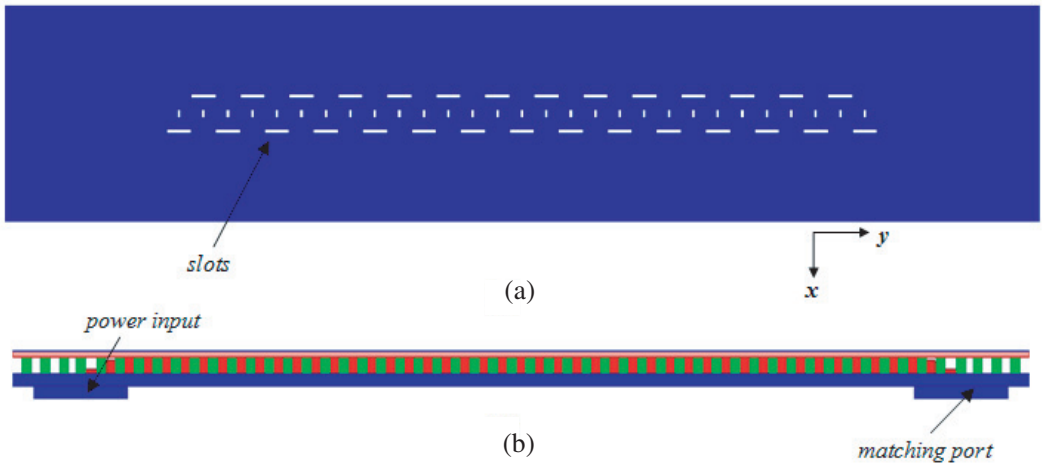

Figure 2. The overall structure of the proposed LWA, (a) the front view; (b) the side view.

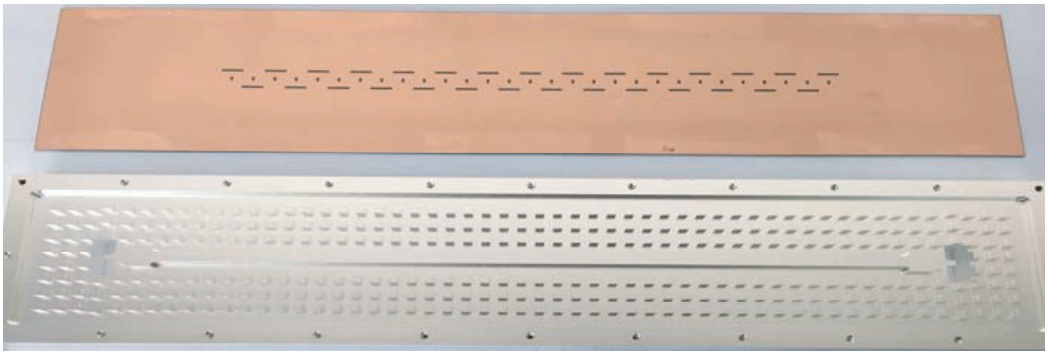

Figure 3. Ridge gap waveguide leaky wave antenna prototype.

3.2. Stopband Design

The dispersion diagram depicts the stopband of RGW transmission line. The size and position of the stopband created by the textured surface are determined by the parameters including the period (p), height (d), width (a) of the pins, and the gap (h). The pin height strongly influences the below cutoff frequency of the stopband. Detailed parameter research is performed in [26]. It should be noted that the two-dimensional (2D) dispersion diagram is acquired when the periodic structure is assumed infinitely long in the propagation direction, besides, without a ridge within the structure. The acquired stopband of this 2D dispersion diagram is from 8.07 GHz to 24.88 GHz shown in Fig. 4, which indicates that fields within this frequency band are prohibited from propagating in the periodic structure.

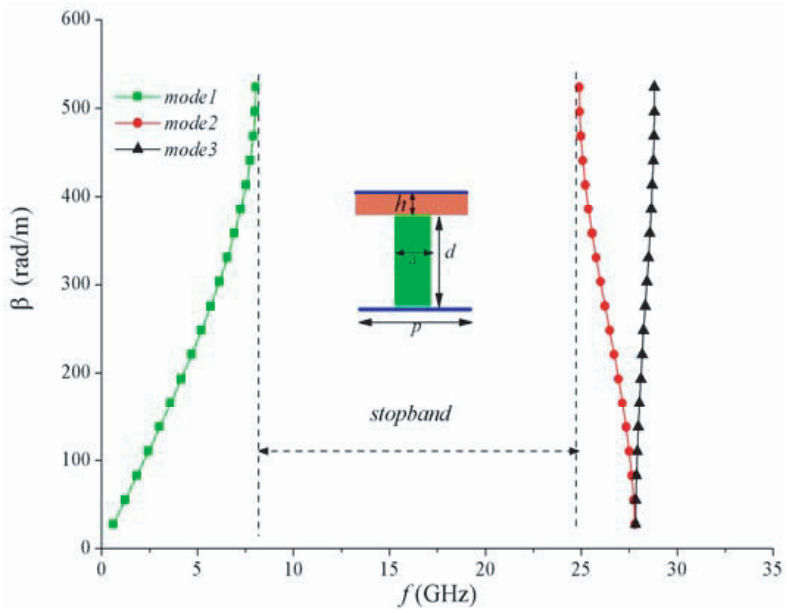

Figure 4. 2D dispersion diagram; pin width $a = 3.0$ mm, pin period $p = 6.0$ mm, pin height $d = 3.0$ mm, gap height $h = 1.0$ mm; the stopband is from 8.07 GHz to 24.88 GHz.

The one-dimensional (1D) dispersion diagram of RGW transmission line depicts the stopband when the confined gap wave propagates along the extended direction of the transmission line. The ridge width is w_f, and the distance between two row metal pins nearest the ridge is w. The result is shown in Fig. 5, in which the stopband is from 11.14 GHz to 17.45 GHz, which meets the requirement referring to operating within the Ku-band (12.5 GHz–17.4 GHz).

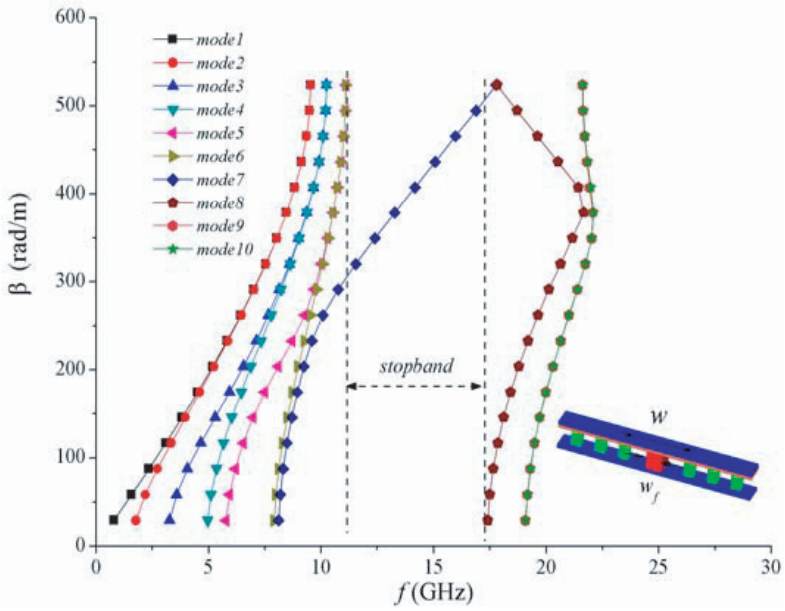

Figure 5. 1D dispersion diagram; $w = 14.0\,\text{mm}$, ridge width $w_f = 4.0\,\text{mm}$; the stopband is from 12.5 GHz to 17.4 GHz.

3.3. Periodic Unit Cell Design

The unit cell of the proposed LWA is illustrated in Fig. 6. There is a transverse slot as a series inductance and a longitudinal slot as a shunt capacitance located on the substrate. The length of the transverse slot is l_{s1} and the width is 1 mm. Similarly, the length and the width of the longitudinal slot are l_{s2} and 1 mm respectively. The dispersion diagram of the unit cell is shown in Fig. 7, which depicts a period phase delay of the unit cell versus frequency explicitly. Based on expression (2), the main lobe direction of the antenna can be calculated. The transition frequency is 14 GHz, at which the main lobe direction is pointing to the broadside. Furthermore, the free-space phase increment is given and compared with

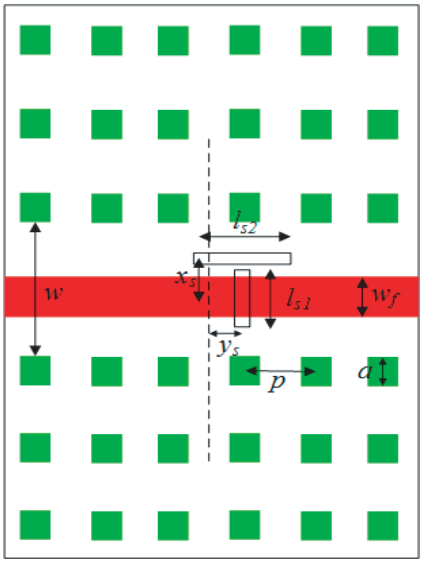

Figure 6. The unit cell of the proposed LWA.

that of the proposed unit cell, which implies the fast wave in RGW transmission line. Fig. 8 provides the normalized attenuation constant versus frequency of the final optimized unit cell structure. The attenuation constant is obtained based on expression (4) in HFSS software. Note that for different slot offsets (y_s) along y axis, the attenuation constant alteration at a single frequency is very small, so the impact on antenna patterns is insignificant. The dimensions of the unit cell are provided in Table 1. It is worth mentioning that the final dimensions are obtained by multiple optimizations. In the optimization process, S-parameters and dispersion diagram of the unit cell should be considered simultaneously.

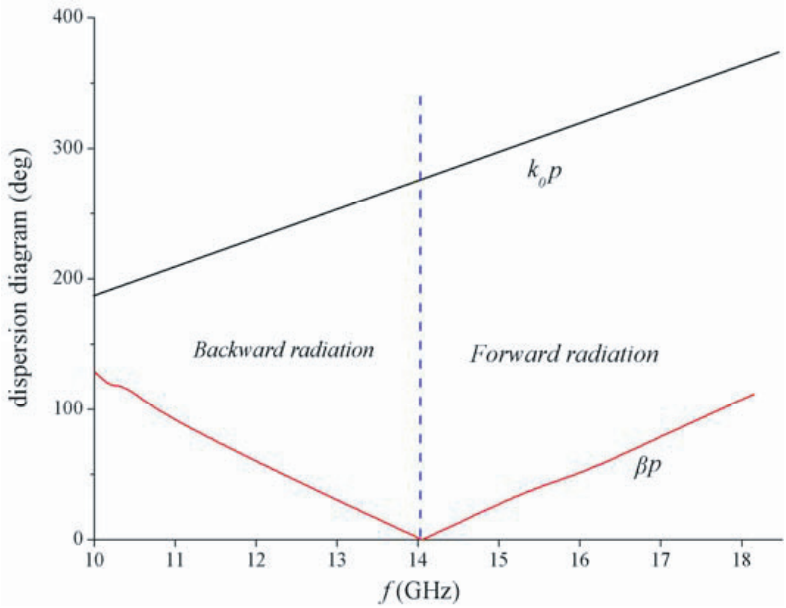

Figure 7. The dispersion diagram of the unit cell.

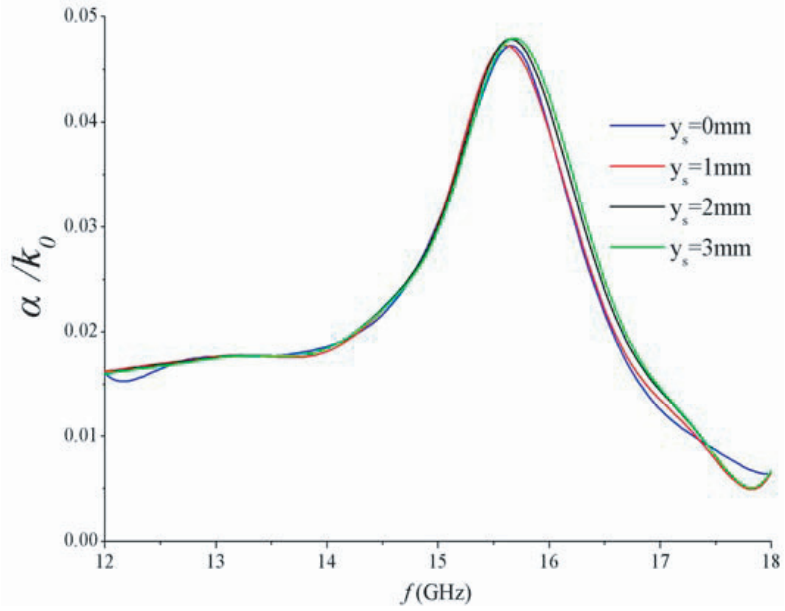

Figure 8. Normalized attenuation constant against frequency.

Table 1. Unit cell structure dimensions (unit: mm).

w	w_f	l_{s1}	l_{s2}	x_s	a	p
14.0	4.0	1.8	7.8	4.0	3.0	6.0

3.4. Transition Design

The feed structure includes the transition from standard rectangular waveguide (WR62) to RGW transmission line for simplicity. This kind of transition usually has wider bandwidth compared to coaxial transition. The details are illustrated in Fig. 9. The stepped impedance transformer transition assures a wide bandwidth that covers the whole Ku-band. The simulated scattering parameter S_{11} is always below -15 dB while S_{21} maintains an excellent conformity about -0.2 dB in the whole Ku-band shown in Fig. 10. This demonstrates that excellent performance has been achieved and the transition meets the requirement completely. The transition dimensions are given in Table 2.

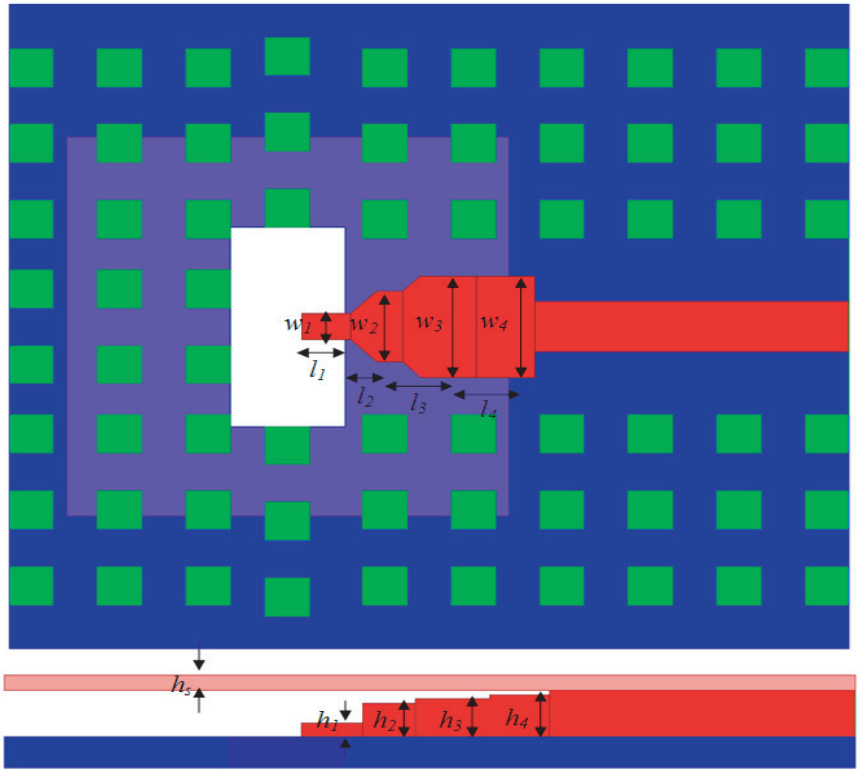

Figure 9. The transition from WR62 to RGW.

Table 2. Transition dimensions (unit: mm).

w_1	w_2	w_3	w_4	l_1	l_2	l_3
2.1	5.6	8.0	8.0	3.3	3.5	5.0
l_4	h_1	h_2	h_3	h_4	h_s	
4.0	0.9	2.2	2.5	2.7	1.0	

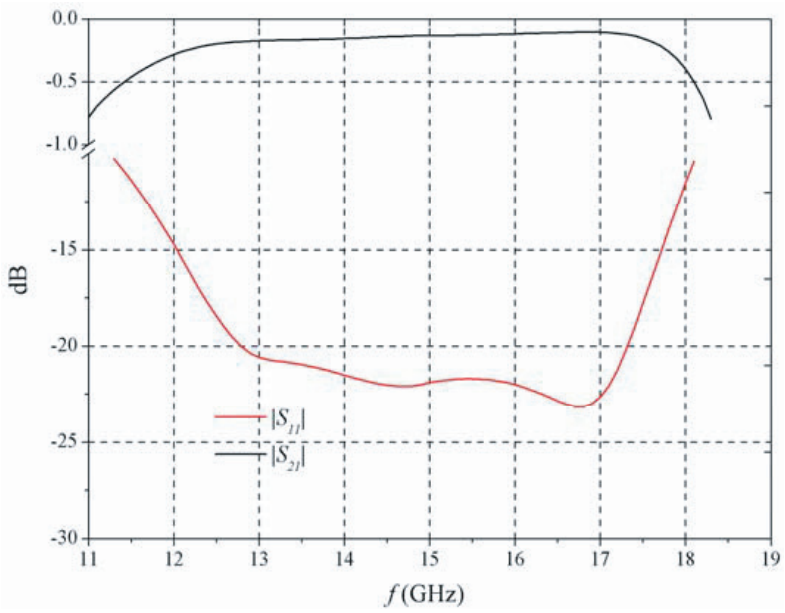

Figure 10. Simulated S-parameters of the transition.

4. RESULTS

The simulated results including S-parameters, gains SLLs, and patterns are provided. For further confirmation, a prototype shown in Fig. 3 is fabricated following the dimensions given in previous sections

Simulated and measured S-parameters of the novel seamless scanning LWA are illustrated in Fig. 11 Measurements are consistent with simulations generally.

Figure 12 illustrates the simulated and measured results of gains and SLLs. The average gain of

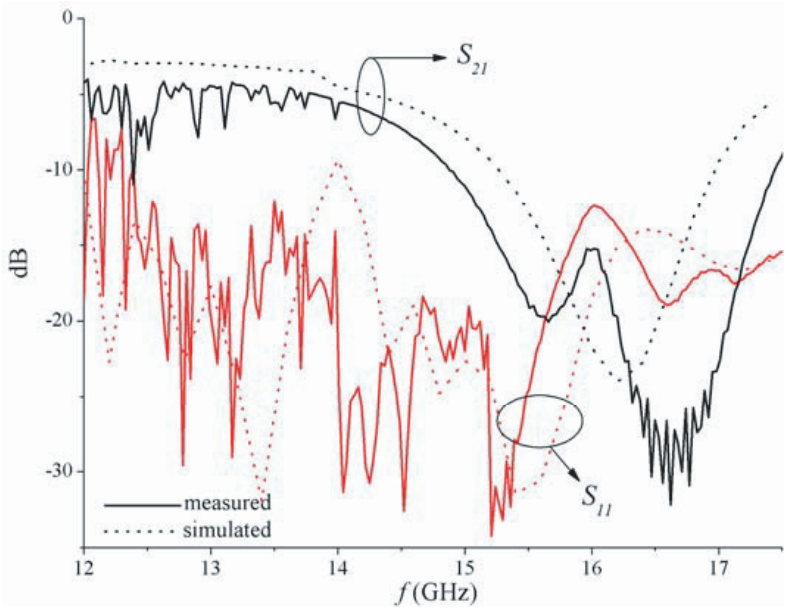

Figure 11. Simulated and measured S-parameters of the proposed LWA.

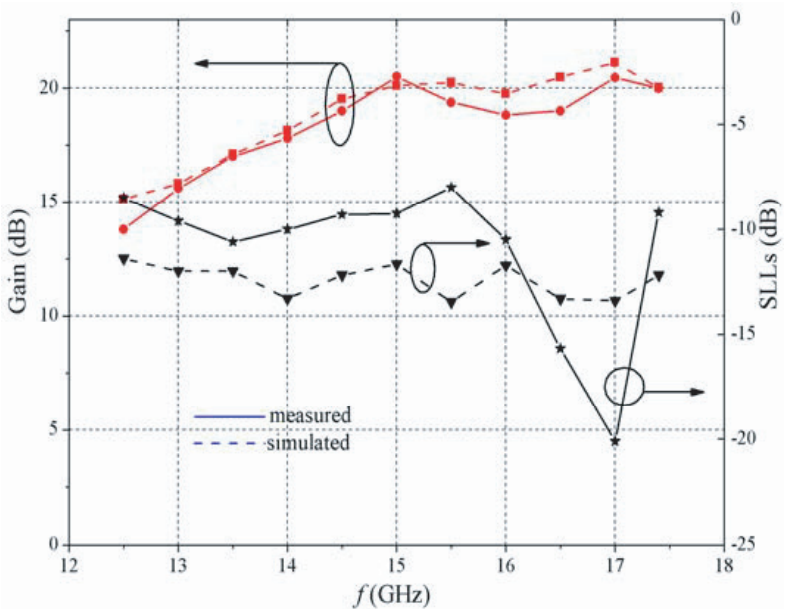

Figure 12. Simulated and measured gains and SLLs.

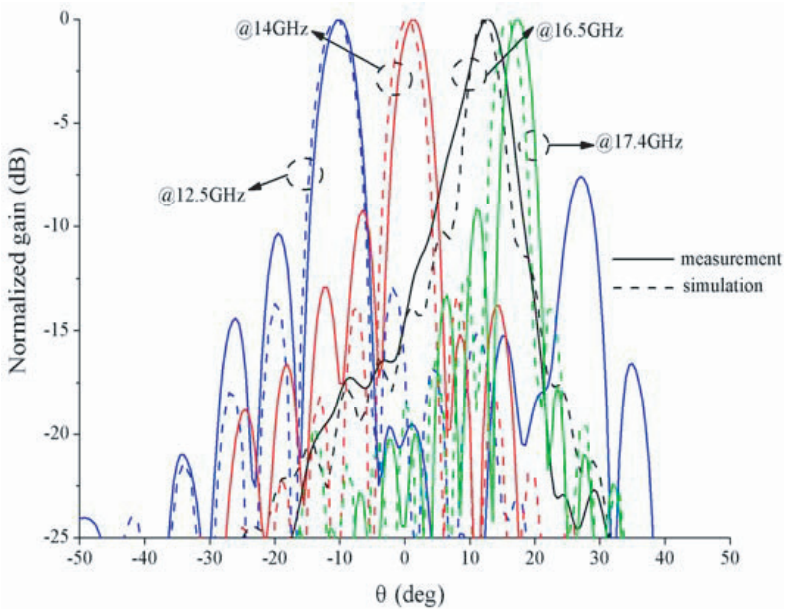

Figure 13. Simulated and measured antenna patterns at 12.5 GHz, 14.0 GHz, 16.5 GHz, and 17.4 GHz.

the designed LWA is 18.3 dB while the maximal gain is 20.45 dB at 17 GHz. The SLLs are acceptable in the frequency band.

Simulated and measured radiation patterns at selected frequencies of the LWA are presented in Fig. 13. It can be seen that good agreements have achieved and the scanning range including broadside radiation is from $-9°$ at 12.5 GHz to $+19°$ at 17.4 GHz. There is a slight shift about the main lobe direction owing to the manufacturing errors.

5. CONCLUSION

A novel seamless scanning LWA in RGW technology is presented. The OSB effect is eliminated by impedance matching technique of the unit cell. A transition from WR62 to RGW transmission line is integrated into the LWA, which meets the requirement referring to operating within the Ku-band. The simulations are supported with measurements and good agreements have been achieved. The bandwidth of the proposed LWA is from 12.5 GHz to 17.4 GHz and the SLLs are acceptable in the frequency band. The scanning range is from $-9°$ to $+19°$ with the average gain of 18.3 dB. These results demonstrate that good performances of this novel antenna have been achieved.

REFERENCES

1. Martinez-Ros, A. J., J. L. Gómez-Tornero, V. Losada, F. Mesa, and F. Medina, "Non-uniform sinusoidally modulated half-mode leaky-wave lines for near-field focusing pattern synthesis," *IEEE Transactions on Antennas and Propagation*, Vol. 63, No. 3, 1022–1031, 2015.
2. Gupta, S., S. Abielmona, and C. Caloz, "Microwave analog Real-Time Spectrum Analyzer (RTSA) based on the spectral-spatial decomposition property of leaky-wave structures," *IEEE Transactions on Microwave Theory and Techniques*, Vol. 57, No. 12, 2989–2999, 2009.
3. Nasimuddin, N., Z. N. Chen, and X. Qing, "Substrate integrated metamaterial-based leaky-wave antenna with improved boresight radiation bandwidth," *IEEE Transactions on Antennas and Propagation*, Vol. 61, No. 7, 3451–3457, 2013.
4. Williams, J. T., P. Baccarelli, S. Paulotto, and D. R. Jackson, "1-D combline leaky-wave antenna with the open-stopband suppressed: Design considerations and comparisons with measurements," *IEEE Transactions on Antennas and Propagation*, Vol. 61, No. 9, 4484–4492, 2013.
5. Nasimuddin, Z. N. Chen, and X. Qing, "Multilayered composite right/left-handed leaky-wave antenna with consistent gain," *IEEE Transactions on Antennas and Propagation*, Vol. 60, No. 11, 5056–5062, 2012.
6. Nasimuddin, Z. N. Chen, and X. Qing, "Dual metamaterials substrate integrated leaky-wave structures for antenna applications," *2012 7th European Microwave Integrated Circuit Conference*, 830–833, 2012.
7. Nasimuddin, Z. N. Chen, and X. Qing, "Tapered composite right/left-handed leaky-wave antenna for wideband broadside radiation," *Microwave & Optical Technology Letters*, Vol. 57, No. 3, 624–629, 2015.
8. Nasimuddin, Z. N. Chen, and X. Qing, "Slotted SIW leaky-wave antenna with improved backward scanning bandwidth and consistent gain," *2017 11th European Conference on Antennas and Propagation (EUCAP)*, 752–755, 2017.
9. Lyu, Y. L., X. X. Liu, P. Y. Wang, D. Erni, Q. Wu, C. Wang, N. Y. Kim, and F. Y. Meng, "Leaky-wave antennas based on noncutoff substrate integrated waveguide supporting beam scanning from backward to forward," *IEEE Transactions on Antennas and Propagation*, Vol. 64, No. 6, 2155–2164, 2016.
10. Mujumdar, M., A. Alphones, and Nasimuddin, "Compact leaky wave antenna with periodical slots on half mode substrate integrated waveguide," *2015 IEEE International Symposium on Antennas and Propagation & USNC/URSI National Radio Science Meeting*, 1740–1741, 2015.
11. Mujumdar, M., A. Alphones, J. Cheng, and Nasimuddin, "Compact leaky wave antenna with periodical slots on substrate integrated waveguide," *The 8th European Conference on Antennas and Propagation (EuCAP 2014)*, 766–770, 2014.
12. Kildal, P. S., "Three metamaterial-based gap waveguides between parallel metal plates for mm/submm waves," *3rd European Conference on Antennas and Propagation 2009, EuCAP 2009*, 28–32, 2009.
13. Kildal, P. S., "Artificially soft and hard surfaces in electromagnetics," *IEEE Transactions on Antennas and Propagation*, Vol. 38, No. 10, 1537–1544, 1990.

14. Zaman, A. U. and P. S. Kildal, "Wide-band slot antenna arrays with single-layer corporate-feed network in ridge gap waveguide technology," *IEEE Transactions on Antennas and Propagation*, Vol. 62, No. 6, 2992–3001, 2014.
15. Polemi, A., S. Maci, and P. S. Kildal, "Dispersion characteristics of a metamaterial-based parallel-plate ridge gap waveguide realized by bed of nails," *IEEE Transactions on Antennas and Propagation*, Vol. 59, No. 3, 904–913, 2011.
16. Kildal, P. S., A. U. Zaman, E. Rajo-Iglesias, E. Alfonso, and A. Valero-Nogueira, "Design and experimental verification of ridge gap waveguide in bed of nails for parallel-plate mode suppression," *IET Microwaves, Antennas & Propagation*, Vol. 5, No. 3, 262–270, 2011.
17. Attia, H., M. S. Sorkherizi, and A. A. Kishk, "60 GHz PRGW slot antenna array with small separation and low mutual coupling," *2015 Global Symposium on Millimeter Waves (GSMM)*, 1–3, 2015.
18. Zarifi, D., A. Farahbakhsh, A. Zaman, and P. S. Kildal, "Design and fabrication of a high-gain 60 GHz corrugated slot antenna array with ridge gap waveguide distribution layer," *IEEE Transactions on Antennas and Propagation*, Vol. PP, No. 99, 1–1, 2016.
19. Alfonso, E., A. U. Zaman, E. Pucci, and P. S. Kildal, "Gap waveguide components for millimetre-wave systems: Couplers, filters, antennas, MMIC packaging," *2012 International Symposium on Antennas and Propagation (ISAP)*, 243–246, 2012.
20. Vosoogh, A. and P. S. Kildal, "High efficiency 2×2 cavity-backed slot sub-array for 60 GHz planar array antenna based on gap technology," *2015 International Symposium on Antennas and Propagation (ISAP)*, 1–3, 2015.
21. Vosoogh, A., A. A. Brazález, and P. S. Kildal, "A V-band inverted microstrip gap waveguide end-coupled bandpass filter," *IEEE Microwave and Wireless Components Letters*, Vol. 26, No. 4, 261–263, 2016.
22. Maaskant, R., W. A. Shah, A. U. Zaman, M. Ivashina, and P. S. Kildal, "Spatial power combining and splitting in gap waveguide technology," *IEEE Microwave and Wireless Components Letters*, Vol. 26, No. 7, 472–474, 2016.
23. Vukomanovic, M., J. L. Vazquez-Roy, O. Quevedo-Teruel, E. Rajo-Iglesias, and Z. Sipus, "Gap waveguide leaky-wave antenna," *IEEE Transactions on Antennas and Propagation*, Vol. 64, No. 5, 2055–2060, 2016.
24. Sharkawy, M. A. and A. A. Kishk, "Long slots array antenna based on ridge gap waveguide technology," *IEEE Transactions on Antennas and Propagation*, Vol. 62, No. 10, 5399–5403, 2014.
25. Mallahzadeh, A. R. and M. H. Amini, "Design of a leaky-wave long slot antenna using ridge waveguide," *IET Microwaves, Antennas & Propagation*, Vol. 8, No. 10, 714–718, 2014.
26. Rajo-Iglesias, E. and P. S. Kildal, "Numerical studies of bandwidth of parallel-plate cut-off realised by a bed of nails, corrugations and mushroom-type electromagnetic bandgap for use in gap waveguides," *IET Microwaves, Antennas & Propagation*, Vol. 5, No. 3, 282–289, 2011.